

# Hydrolysis–condensation reactions of TEOS in the presence of acetic acid leading to the generation of glass-like silica microspheres in solution at room temperature

Goutam De,\* Basudeb Karmakar and Dibyendu Ganguli

Sol–Gel Division, Central Glass and Ceramic Research Institute, 196 Raja S. C. Mullick Road, Jadavpur, Calcutta, 700 032, India. E-mail: gde41@hotmail.com

Received 20th April 2000, Accepted 31st July 2000

First published as an Advanced Article on the web 5th September 2000

The generation of dense silica microspheres (density  $2.14 \pm 0.02 \text{ g cm}^{-3}$ ; 95–98% of theoretical value) from the hydrolysis and condensation reactions of  $\text{Si}(\text{OC}_2\text{H}_5)_4$  (TEOS) in the presence of a fixed concentration of acetic acid and water (TEOS :  $\text{CH}_3\text{COOH}$  :  $\text{H}_2\text{O}$  = 1 : 4 : 4) were studied by FTIR absorption spectroscopy, particle size measurement by dynamic light scattering and transmission electron microscopy. The growth of ethanol peaks at  $1049 \text{ cm}^{-1}$  (C–O stretch) and  $882 \text{ cm}^{-1}$  (C–C stretch), as well as the absorbance decrease of an alkoxide peak at  $792 \text{ cm}^{-1}$  ( $\text{SiO}_4$  asymmetric stretch +  $\text{CH}_2$  rock) during the hydrolysis–condensation process followed a first order reaction with the rate constant ( $k$ ) within the range  $6\text{--}10 \times 10^{-3} \text{ s}^{-1}$ . The formation of silica particles and their growth in the sol *via* condensation reactions of silanols and subsequent molecular addition were monitored by measuring the particle size profile with respect to time. This study confirmed the generation of nano-sized primary particles of dimensions about 50 nm, which gradually grew to 2000–3000 nm dense particles at the end of the reaction. The particle size data were further confirmed by TEM investigations.

## 1. Introduction

Synthesis of silica microspheres from acid or base hydrolysis–condensation reactions of  $\text{Si}(\text{OC}_2\text{H}_5)_4$  (TEOS) has been reported by several authors.<sup>1–15</sup> The dense, highly pure glassy silica microspheres have various applications in clinical, biomedical<sup>16,17</sup> and electronic packaging fields.<sup>18</sup> It has been observed by us<sup>11</sup> that dense, glassy silica spheres could be obtained directly from the sol as the final product of hydrolysis–condensation reactions of TEOS in the presence of any acid (inorganic or organic) and water at room temperature. The pH and  $\text{H}_2\text{O}/\text{TEOS}$  molar ratio are the controlling factors governing the formation of these dense spheres. Furthermore, we have also noticed a molar ratio narrowed regime in the ternary system TEOS– $\text{CH}_3\text{COOH}$ – $\text{H}_2\text{O}$ , particularly suitable for obtaining monodisperse dense spherical silica powders.<sup>11</sup> In this regime the best composition is TEOS :  $\text{CH}_3\text{COOH}$  :  $\text{H}_2\text{O}$  = 1 : 4 : 4 (molar), and when the three constituents are mixed, dense spherical silica particles separate out from the sol at room temperature. Stirring (with a magnetic stirring bar) has a pronounced effect on the particle size, and we noticed that in the presence of stirring, particles ranging in size from 20 to 40  $\mu\text{m}$  were formed, whereas the absence of stirring resulted in the generation of much smaller particles of average size 0.8  $\mu\text{m}$ .<sup>11</sup> It must be pointed out that the formation (TEOS– $\text{CH}_3\text{COOH}$ – $\text{H}_2\text{O}$  system) and characteristics (micrometer size, high density) of such spheres as a product of hydrolysis–condensation of silicon alkoxide are different from those observed in the case of silica spheres obtained from ammoniacal TEOS solutions (Stöber process),<sup>1</sup> spherical silica obtained from highly acidic solutions of TMOS (tetramethoxyorthosilicate)<sup>8</sup> and recently reported porous spherical silica particles obtained by emulsion techniques.<sup>14,15</sup>

In the Stöber process,<sup>1</sup> the formation of spherical, monodisperse, monosize porous silica particles from ammoniacal TEOS solutions was explained by the formation of silica nuclei which aggregate to form particles. Sakka and Kozuka<sup>8</sup> showed, in a series of papers, that spherical silica particles could be obtained from highly acidic TMOS solutions. The density of

these particles is well below the theoretical density of silica. In this case they used molar ratios corresponding to  $\text{HCl}/\text{TMOS}$  = 0.4 and  $\text{H}_2\text{O}/\text{TMOS}$  = 1.53. They explained these particles to have formed *via* folding of linearly polymerized primary groups into round-shaped secondary particles which had unhydrolyzed alkoxy groups. This mechanism was postulated because the low  $\text{H}_2\text{O}/\text{TMOS}$  ratio favoured the formation of linear polymers. In a similar type of reaction Kawaguchi and Ono<sup>6</sup> reported the preparation of relatively dense silica spheres from the TEOS– $\text{HNO}_3$ – $\text{H}_2\text{O}$  system ( $\text{H}_2\text{O}/\text{TEOS}$  < 2). They explained the formation of spheres as a result of the formation of an emulsion in the water–alkoxide immiscible system, in which water formed tiny droplets because of stirring; TEOS reacted with water through the spherical interface, and in the presence of  $\text{HNO}_3$ , giving rise to fully hydrolyzed and polymerized products which retained the shape of the original spherical droplets. Among the above different processes, only the mechanism of the Stöber process (ammoniacal TEOS) is well understood.<sup>9,10</sup> The mechanisms of the other processes (acidic TEOS) are not clear.

In this paper an attempt has been made to trace the reaction pathways involved in the formation of dense silica spheres through an acidic TEOS system with the help of FTIR and dynamic light scattering studies. The rate of hydrolysis–condensation reaction of TEOS in the presence of a fixed concentration of acetic acid–water, leading to the formation of glass-like silica microspheres (density  $2.14 \pm 0.02 \text{ g cm}^{-3}$ ; 95–98% of theoretical density) was studied from the evolution of FTIR absorption peaks of alkoxide and ethanol with time. The growth of silica spheres was followed by measuring the particle size profile using the dynamic light scattering method with respect to time and by transmission electron microscopy.

## 2. Experimental

### 2.1 Synthesis

TEOS (Fluka, purum grade) was added to a mixture of acetic acid (Analar grade, BDH) and water (double distilled) under

stirring at  $26 \pm 1^\circ\text{C}$ . The stirring was continued for 1 min. The molar composition of  $\text{TEOS}:\text{CH}_3\text{COOH}:\text{H}_2\text{O}$  was 1:4:4. On standing, the solution became cloudy after about 400 s and dense spherical silica powders were separated and settled down after about 600 s. The powders could be separated by filtration.

## 2.2 FTIR

The hydrolysis–condensation reactions were monitored by FTIR absorption spectroscopy at room temperature ( $26^\circ\text{C}$ ) with a Nicolet 5 PC spectrometer using  $2.0\text{ cm}^{-1}$  resolution. For this study, the sol after mixing the reactants was quickly placed in between two KBr windows separated by an annular Teflon ring spacer of thickness 0.05 mm. The FTIR absorbance spectra of this 0.05 mm thin layer sol were recorded after every 60 s up to 640 s.

## 2.3 Dynamic light scattering (DLS)

The formation of particles in the sol and their size distribution were monitored by the dynamic light scattering method using a helium–neon laser with a Malvern particle size analyzer (model autosizer IIc) at room temperature ( $26 \pm 1^\circ\text{C}$ ). For this measurement, the sol after about 1 min of stirring was poured in a standard 1 cm polypropylene cuvette and placed in the sample compartment of the instrument and the data were recorded every 30 s up to 670 s.

## 2.4 TEM

TEM investigations of the intermediate and final samples were obtained by using a JEOL TEM-200CX instrument. The intermediate particles were obtained by arresting the reactions with the addition of acetone at different time schedules following the particle size analyser data.

Density of the dried ( $150^\circ\text{C}$ ) silica spheres was determined by the Archimedes principle. Thermogravimetric analysis was performed with a Shimadzu DT50 instrument. The BET surface area and  $\text{N}_2$  adsorption–desorption isotherm of the samples were measured with a Quantachrome Autosorb 1 instrument.

## 3. Results and discussion

### 3.1 General

The average density of dried ( $150^\circ\text{C}$ , 16 h) spherical silica powders (obtained after the end of the reaction after washing twice with ethanol followed by acetone) was measured by the Archimedes principle and found to be  $2.14 \pm 0.02\text{ g cm}^{-3}$ . The  $\text{N}_2$  adsorption experiment of the powder samples was carried out after degassing at  $150^\circ\text{C}$  for 16 h. Fig. 1 shows the  $\text{N}_2$  adsorption–desorption isotherm data of the above powders. The typical type II isotherm indicates that the material is non-porous.<sup>19</sup> Furthermore, the multipoint BET surface area obtained by  $\text{N}_2$  adsorption showed a very low value, *i.e.* of

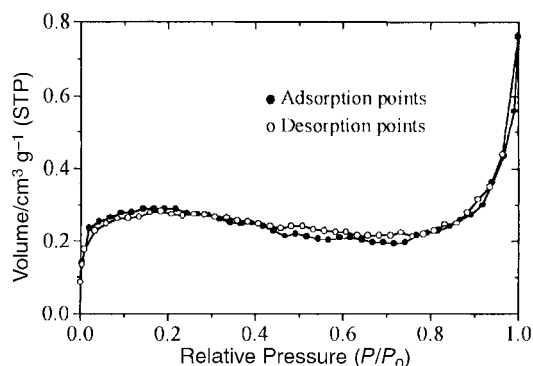


Fig. 1  $\text{N}_2$  adsorption–desorption isotherm of silica microspheres.

the order of  $<1\text{ m}^2\text{ g}^{-1}$ . Diffuse reflectance FTIR spectra of these dense-as-prepared particles showed the absence of both acetate and alkoxy groups. However, the FTIR spectrum shows the presence of silanol ( $\text{Si-OH}$ ) vibrations at  $950\text{ cm}^{-1}$ . Thermogravimetry (rate of heating  $10^\circ\text{C min}^{-1}$ ) of the above powders showed only about 5% weight loss up to about  $500^\circ\text{C}$  due to elimination of absorbed water and water formed due to condensation of silanols,<sup>20,21</sup> and almost no weight loss was observed after heating from  $500^\circ\text{C}$  up to  $1200^\circ\text{C}$ . FTIR spectra of the corresponding  $500^\circ\text{C}$  heated powders showed no absorption due to silanol ( $\text{Si-OH}$ ) vibrations. All the above data lead to the conclusion that the silica microspheres formed in the solution were highly dense, almost glass-like silica.

## 3.2 FTIR

The series of FTIR spectra of the sol at different stages of reaction provide interesting information (Fig. 2) which is summarized below:

(i) The spectrum at 100 s (Fig. 2a) was characterized mainly by strong bands at  $1105$ ,  $1080$  and  $961\text{ cm}^{-1}$  and medium to weak bands at  $1170$ ,  $792$  and  $478\text{ cm}^{-1}$ , all attributed to TEOS, bands at  $1013$ ,  $620$  and  $458\text{ cm}^{-1}$  due to acetic acid and bands at  $1049$  and  $882\text{ cm}^{-1}$  due to ethanol. Additional strong bands for acetic acid were also recorded at around  $1725$ ,  $1394$  and  $1280\text{ cm}^{-1}$  (not shown in the spectral range covered in Fig. 2).

(ii) With increasing time of reaction, the TEOS bands experienced a strong decrease in intensity, while the intensity of the  $1049$  and  $882\text{ cm}^{-1}$  bands due to alcohol gradually increased up to 460 s and remained constant thereafter. It is interesting to note that the absorbance values of the  $\text{Si-O-C}$  stretching bands of TEOS<sup>22,23</sup> at  $1105$  and  $1080\text{ cm}^{-1}$  suddenly increased with time of reaction from 100 s to 160 s with a slight blue shift (Fig. 2a), which may be due to the change in the dipole moment of the  $\text{Si-O-C}$  vibration upon acid ( $\text{H}^+$ ) attack during hydrolysis.

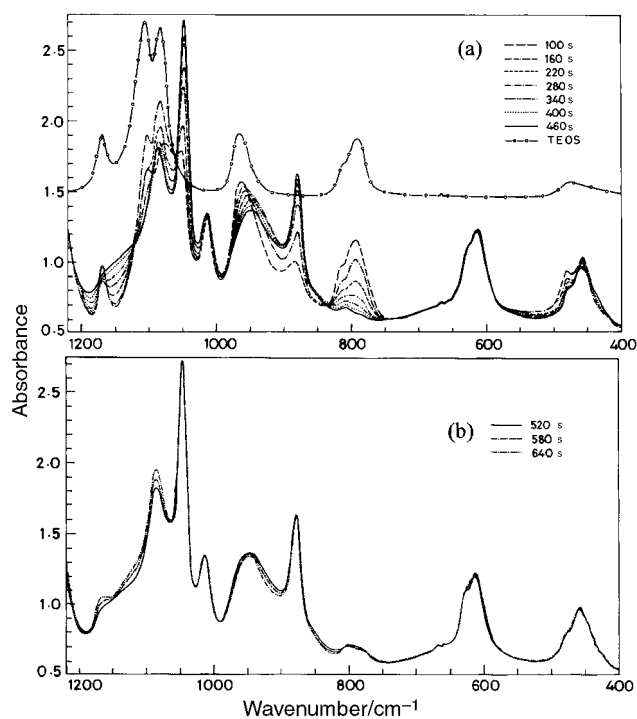
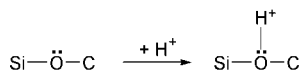


Fig. 2 FTIR absorption spectra of the  $\text{TEOS-CH}_3\text{COOH-H}_2\text{O}$  mixture at various times after mixing: (a) 100–460 s and (b) 520–640 s. The spectrum of TEOS is shown for comparison (absorbance scale of TEOS spectrum is arbitrary).

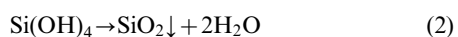
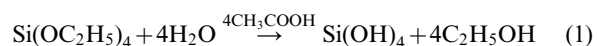


(iii) By around 400 s, peaks for the alkoxy groups ( $-\text{OC}_2\text{H}_5$ ) of TEOS disappeared almost completely and as a consequence the TEOS peaks at 1170 ( $\text{CH}_3$  rock), 1105 ( $\text{C}-\text{O}$  asym. stretching) and  $792\text{ cm}^{-1}$  ( $\text{SiO}_4$  asym. stretching +  $\text{CH}_2$  rock) were absent. Simultaneous growth of the band at about  $950\text{ cm}^{-1}$  indicated the formation of  $\text{Si}-\text{OH}$  (silanol) groups. The peaks appearing at about  $1165\text{ cm}^{-1}$  (longitudinal optic (LO) component of  $\text{Si}-\text{O}-\text{Si}$  asym. stretching<sup>24,25</sup>) and  $805\text{ cm}^{-1}$  ( $\text{Si}-\text{O}-\text{Si}$  sym. stretching<sup>24,25</sup>) were due to the formation of the  $\text{Si}-\text{O}_4$  network of  $\text{SiO}_2$  (Fig. 2b). The  $\text{Si}-\text{O}-\text{Si}$  asymmetric stretching band of  $\text{SiO}_2$  overlapped with the alcohol bands (appearing at about  $1090\text{ cm}^{-1}$ ).

(iv) Bands due to acetic acid ( $1013$ ,  $620$  and  $458\text{ cm}^{-1}$ ) remained virtually unchanged during the course of the reaction.

(v) The most interesting feature of the series of spectra obtained at 100–400 s is that their superimposition revealed several crossovers at specific wavenumbers (mainly at  $1116$ ,  $1057$ ,  $835\text{ cm}^{-1}$ ), recognized as isosbestic points<sup>26</sup> (Fig. 2a). The absorbance values at these points remained constant when reactants and product composition changed with time.

FTIR studies of the above hydrolysis–condensation reactions of TEOS showed the following stages: (i) depletion of alkoxy molecules followed by (ii) production of alcohol and (iii) formation of  $\text{SiO}_2$ . The overall hydrolysis of TEOS and subsequent dehydration of the product formed may be summarized in eqn. (1) and (2):



The above series of FTIR spectra (Figs. 2a and b) clearly showed that during the course of the reaction ethanol molecules gradually formed at the expense of alkoxy and as a consequence the intensities of the ethanol peaks increased whereas the intensities of the alkoxy peaks decreased with time. The rate of the hydrolysis reaction (eqn. (1)) is obtained by measuring the absorbance values of the alkoxy peak at  $792\text{ cm}^{-1}$  and the alcohol peaks at  $882$  ( $\text{C}-\text{C}$  stretch) and  $1049\text{ cm}^{-1}$  ( $\text{C}-\text{O}$  stretch). These peaks are chosen because no overlap of bands is found in these regions. It has been found that the plots (Fig. 3) of  $-\log(A_t - A_\infty)$  vs. time (Fig. 3a,

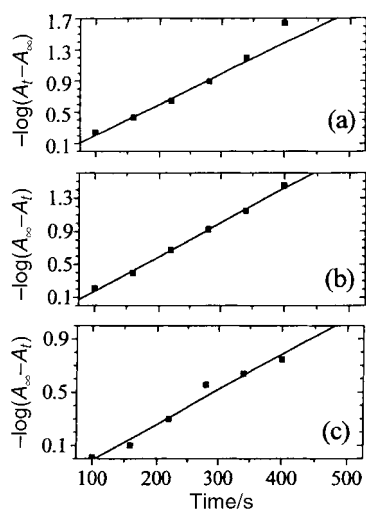


**Fig. 3** Plots of (a):  $-\log(A_t - A_\infty)$  vs. time for the TEOS peak appearing at  $792\text{ cm}^{-1}$ ; (b) and (c):  $-\log(A_\infty - A_t)$  vs. time for the ethanol peaks appearing at  $882$  and  $1049\text{ cm}^{-1}$  respectively (see Fig. 2).

alkoxide peak) and  $-\log(A_\infty - A_t)$  vs. time (Figs. 3b and c, alcohol peaks) showed straight lines at least up to 400 s which indicates that the process followed a first order reaction.  $A_\infty$  and  $A_t$  are the absorbance values at times infinity and  $t$  respectively. The rate constant ( $k$ ) values calculated from the slopes of Figs. 3a, b and c are  $10 \times 10^{-3}\text{ s}^{-1}$ ,  $9 \times 10^{-3}\text{ s}^{-1}$ , and  $6 \times 10^{-3}\text{ s}^{-1}$ , respectively. It is concluded therefore that under these particular conditions (*i.e.* in the presence of 4 moles of acetic acid and water at a constant temperature) TEOS hydrolyzes at a rate of  $(8 \pm 2) \times 10^{-3}\text{ s}^{-1}$ . It is expected that under these conditions, *i.e.* low pH ( $\approx 1.63$ ) and high water content ( $\text{H}_2\text{O}/\text{TEOS} = 4$ ), the rate of hydrolysis would be high compared to that of condensation<sup>21,27,28</sup> and we might expect that hydrolysis will be essentially complete at an early stage of reaction. In fact, in this case within about 340–400 s the hydrolysis reaction (some condensation reactions must have also occurred simultaneously during the latter stage of hydrolysis as shown by the formation of unstable, large-sized polymeric units after 280 s; see section 3.3) was essentially complete; most of the condensation reactions occurred after this stage, resulting in the generation of silica particles. The occurrence of isosbestic points in the spectra obtained up to about 400 s strongly indicates a reaction (in this case eqn. (1)) in which the products should remain at a constant ratio till its completion.<sup>26</sup>

It has been mentioned above that the intensities of the 1105 and  $1080\text{ cm}^{-1}$  peaks due to  $\text{Si}-\text{O}-\text{C}$  (TEOS) stretching<sup>22,23</sup> initially increased due to acid attack and then gradually decreased due to hydrolysis up to 400 s; after this, the intensity again started to increase due to the formation of more and more  $\text{Si}-\text{O}-\text{Si}$  bonds by condensation (Fig. 2b). Parallel to this, the appearance of peaks at about  $1165\text{ cm}^{-1}$  (LO component of  $\text{Si}-\text{O}-\text{Si}$  asym. stretching) and  $805\text{ cm}^{-1}$  ( $\text{Si}-\text{O}-\text{Si}$  sym. stretching) at this stage supports the above condensation. The intensities of the latter bands were further increased due to the growth and formation of a glass like structure.

### 3.3 Dynamic light scattering (DLS)

To observe the formation and growth of silica particles, a set of experiments was performed by *in-situ* generation of particles in the sample chamber of a particle size analyzer by dynamic light scattering (DLS) with time (Table 1, Fig. 4). It showed the formation of a small number of large unstable polymeric units of the order of 2000–3000 nm in size in the initial stages (280 s). Before 280 s DLS showed no detectable particles. At that stage the sol remained almost transparent. These unstable large polymeric units quickly decomposed into relatively stable smaller particles (up to 520 s). After this period of time these small particles (diameter about 50 nm) started to grow in size; at the end of reaction (670 s) dense spherical particles of about

**Table 1** Dynamic light scattering (DLS) data<sup>a</sup> on typical experimental results

Time/s	Average particle diameter/nm	Count rate/s <sup>-1</sup>
280	2006	11900
340	587	18300
400	124	50400
430	114	64600
460	86	78700
490	80	88000
520	52	93200
550	54	97500
580	60	100700
610	211	100700
640	341	100000
670	2363	105700

<sup>a</sup>No particles were detected before 280 s.

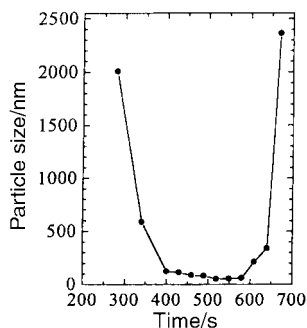


**Fig. 4** Dynamic light scattering data showing the evolution of silica particles with respect to time.

2500 nm diameter were separated from the mother sol. These results are presented in Fig. 4.

The initial stage of the reactions may be due to the formation of some interconnected polymeric network during the acid attack of the hydrolysis reaction. DLS showed the existence of large polymeric units at 280 s. These units are small in number and we obtained irreproducible results (count rate varied from 3000 to 10 000  $s^{-1}$ ; the size varied significantly from 2000 to 3000 nm) from experiment to experiment. Further, the transparency of the sol indicated that their refractive index was close to that of the mother sol itself; as a result they were not visible. At about 400 s the sol became cloudy, indicating the existence of solid silica particles in the sol. It has been observed that during depolymerization of the unstable large polymers into smaller ones, the count rate gradually increased, indicating a progressive increase in the number of particles in the sol. Once the smallest particles (520 s, 52 nm) were formed, the count rate remained almost constant during the growth (550–670 s) of these particles (Table 1, Fig. 4). It is well known that the homogeneous nucleation and growth of precipitates involves two basic steps. From a homogeneous liquid, solids are generated in a process referred to as nucleation. Once formed, the solid particles increase in size by molecular addition where soluble species deposit on the solid surface, or by aggregation with other particles. Molecular addition should not increase the number of particles while aggregation of smaller units results in a decrease in numbers.

Our results indicate that the growth of the particles occurred due to molecular addition and the small particles (about 50 nm) of high surface charge (low pH) acted as nuclei. This conclusion is derived from the supposition that, had the growth occurred *via* the aggregation of small particles (52 nm) formed at 520 s, the count rate would have decreased. It may also be pointed out that the yield (wt. of dried silica powder  $\times$  100/total calculated silica amount present in the sol) of this process is about 35%, so it is quite likely that the large amount of soluble silica present in the sol could easily be deposited on to the small nuclei having high surface charge.

It may be further noted that in the light scattering experiment, small numbers of large polymeric units (simultaneous hydrolysis–condensation product) were observed at about 280 s after mixing, but in the IR spectra the Si–O–Si vibrations (at about 1165 and 805  $cm^{-1}$ ) were not detectable or were interfered with, due to the presence of unhydrolyzed ethoxy groups which absorb in these regions. The presence of these small numbers of unstable units (precursor polymer entity) at the very beginning indicates that the condensation reaction had already begun at 280 s. However, in spite of the large size of these units (2000–3000 nm) they were not visually noticeable, which indicated that they were probably soluble polymeric products and had a refractive index similar to that of the solvent liquid. Thus such unstable polymeric units stand, in our opinion, apart from the much smaller powder products which started appearing after 400 s of reaction.

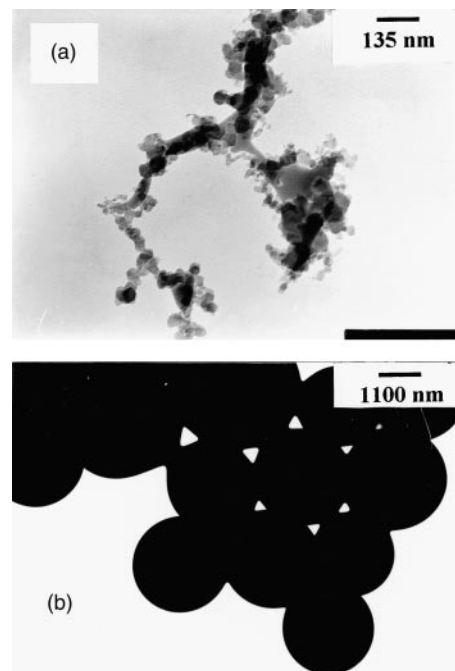


**Fig. 5** TEM images showing the growth of silica spheres. Samples taken from the TEOS–CH<sub>3</sub>COOH–H<sub>2</sub>O mixture after (a) 460 s and (b) 670 s.

### 3.4 TEM

TEM pictures of the particles obtained 460 and 670 s after mixing (at 26 °C) are shown in Figs. 5a and b. It has been observed that after 460 s of reaction (Fig. 5a) particles of the order of 60 nm are present, which supports the particle size data shown in Fig. 4. The cementing material binding the particles together is identified as the solidification product of the silica-rich mother liquid. The large particles of about 2500 nm (Fig. 5b) were generated as the condensation product after 670 s. Fig. 5b shows the presence of agglomerated particles. However, TEM images of the washed (twice with ethanol followed by acetone) and air dried (150 °C) powders shows unagglomerated spherical particles (Fig. 6).

## 4. Conclusion

Hydrolysis and condensation reactions of Si(OC<sub>2</sub>H<sub>5</sub>)<sub>4</sub> in the presence of acetic acid and water (in 1:4:4 molar ratios) leading to the formation of dense silica microspheres were monitored by FTIR absorption spectroscopy, particle size measurement by dynamic light scattering and transmission electron microscopy. The rate of absorbance decrease of the non-interfered alkoxide peak and the corresponding absorbance increase of the ethanol peaks in FTIR spectra during the hydrolysis–condensation process were found to indicate first order reactions. The generation of silica particles as the

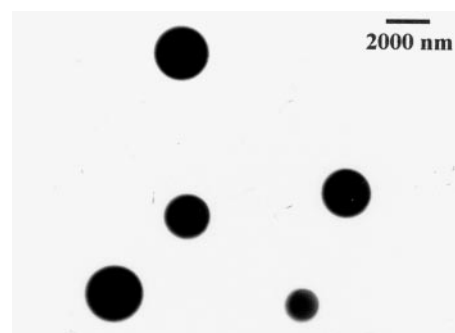


**Fig. 6** TEM image showing monodisperse silica spheres.

reaction product was preceded by the transient formation of large silicate polymeric units as shown by dynamic light scattering, which broke down to about 50 nm units after 500 s; these units grew to 2000–3000 nm dense spherical silica particles at the end of the reaction.

### Acknowledgement

We thank Dr. D. Kundu of this institute for helpful suggestions.

### References

- 1 W. Stöber, A. Fink and E. Bohn, *J. Colloid Interface Sci.*, 1968, **26**, 62.
- 2 M. D. Sacks and T. Tseung-Yuen, *J. Am. Ceram. Soc.*, 1984, **67**, 526.
- 3 G. H. Bogush and C. F. Zukoski IV, in *Ultrastructure Processing of Advanced Ceramics*, ed. J. D. Mackenzie and D. R. Ulrich, Wiley, New York, 1988, p. 477.
- 4 E. C Ruvolo Jr., H. L. Bellinetti and M. A. Aegerter, *J. Non-Cryst. Solids*, 1990, **121**, 244.
- 5 M. T. Harris, R. R. Brunson and C. H. Byers, *J. Non-Cryst. Solids*, 1990, **121**, 397.
- 6 T. Kawaguchi and K. Ono, *J. Non-Cryst. Solids*, 1990, **121**, 383.
- 7 R. Masuda, W. Takahasi and M. Ishii, *J. Non-Cryst. Solids*, 1990, **121**, 389.
- 8 H. Kozuka and S. Sakka, *Chem. Mater.*, 1989, **1**, 398; J. Yamaguchi, H. Kozuka and S. Sakka, *Trans. Mater. Res. Soc. Jpn.*, 1990, **1**, 140.
- 9 G. H. Bogush and C. F. Zukoski IV, *J. Colloid Interface Sci.*, 1991, **142**, 1.
- 10 G. H. Bogush and C. F. Zukoski IV, *J. Colloid Interface Sci.*, 1991, **142**, 19.
- 11 B. Karamkar, G. De, D. Kundu and D. Ganguli, *J. Non-Cryst. Solids*, 1991, **135**, 29; B. Karamkar, G. De and D. Ganguli, *J. Non-Cryst. Solids*, 2000, **272**, 119.
- 12 A. van Blaaderen, J. van Geest and A. Vrij, *J. Colloid Interface Sci.*, 1992, **154**, 481.
- 13 M. K. Titulaer, J. B. H. Jansen and J. W. Gens, *J. Non-Cryst. Solids*, 1994, **168**, 1.
- 14 H. Izutsu, F. Mizukami, P. K. Nair, Y. Kiyozumi and K. Maeda, *J. Mater. Chem.*, 1997, **7**, 767.
- 15 Q. Huo, J. Feng, F. Schuth and G. D. Stucky, *Chem. Mater.*, 1997, **9**, 14.
- 16 G. M. Motes-G., R. A. Draughn and T. H. Simpson, Jr., in *Biomedical Materials*, ed. J. M. Williams, M. F. Nichols and W. Zings, Materials Research Society, Pennsylvania, 1986, p. 97.
- 17 M. Taira and M. Yamaki, *J. Mater. Sci., Mater. Med.*, 1995, **6**, 197.
- 18 O. Nakagawa, I. Sasaki, H. Hamamura and H. Banjo, *J. Electron. Mater.*, 1984, **13**, 231.
- 19 S. J. Gregg and K. S. Sing, *Adsorption, Surface area and Porosity*, Academic Press, London, 1967.
- 20 G. De, D. Kundu, B. Karmakar and D. Ganguli, *J. Non-Cryst. Solids*, 1993, **155**, 253.
- 21 L. L. Hench and J. K. West, *Chem. Rev.*, 1990, **90**, 33.
- 22 A. Lee Smith, *Spectrochim. Acta*, 1960, **16**, 87.
- 23 N. B. Colthup, L. H. Daly and S. E. Wiberley, *Introduction to Infrared and Raman Spectroscopy*, 3rd edn., Academic Press, Boston, 1990, p. 361.
- 24 R. V. Adams and R. W. Douglas, *J. Soc. Glass Technol.*, 1959, **43**, 147.
- 25 A. Duran, C. Serna, V. Fornes and J. M. Fernandez Navarro, *J. Non-Cryst. Solids*, 1986, **82**, 69.
- 26 R. G. Wilkins, *The Study of Kinetics and Mechanism of Transition Metal Complexes*, Allyn and Bacon Inc., Boston, 1974.
- 27 C. J. Brinker and G. W. Scherer, *Sol-Gel Science*, Academic Press Inc., Boston, 1990, p. 212.
- 28 M. Prassas and L. L. Hench, in *Ultrastructure Processing of Ceramics, Glasses and Composites*, ed. L. L. Hench and D. R. Ulrich, Wiley, New York, 1984, p. 100.